Calibration and Validation Site characterisation for INSAT-3D Satellite over Great Rann of Kutch and White Rann of Kutch

Joint Campaign of SAC & IMD
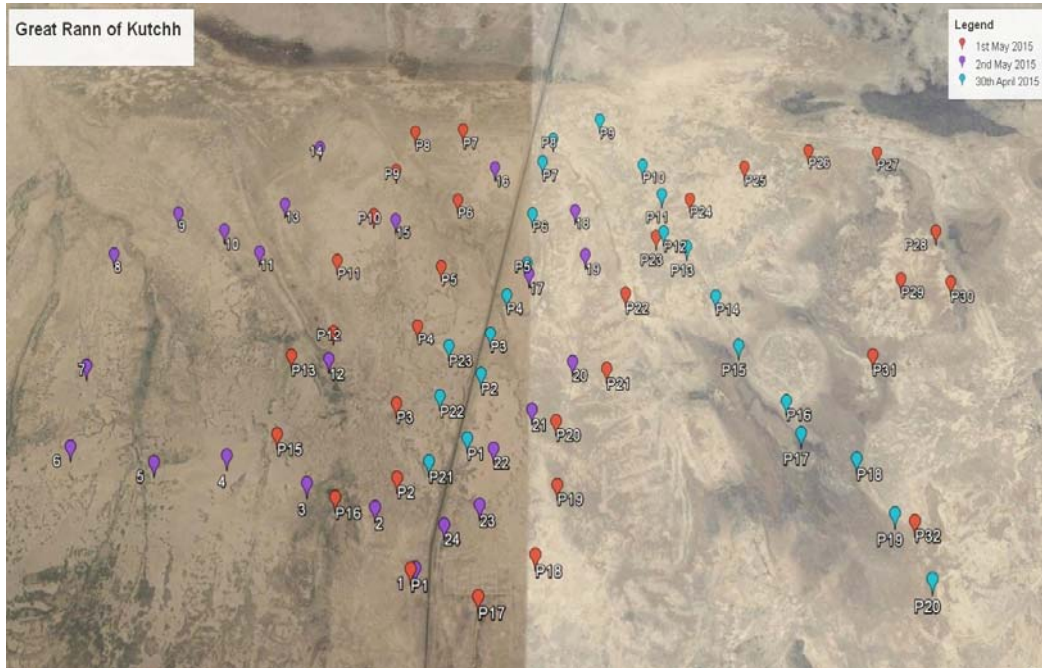
May-2015

**Calibration and Validation Division
Atmosphere and Oceanic Data Archival, Validation and
Dissemination Group, EPSA
Space Applications Centre (ISRO)
Ahmedabad**

Calibration and Validation Team:

❖ *SAC-ISRO*

   1) *Hiren Bhatt*
   2) *R. P. Prajapati*
   3) *Piyushkumar N Patel*

❖ *IMD-Delhi*

   1) *A K Sharma*
   2) *A K Mitra*

❖ *IMD-Bhuj Office*

   1) *Rakesh Kumar*
   2) *D. M. Hindia*
   3) *K. C. Modh*

Document control sheet

1. Report No.	SAC/EPSA/ADVG/CVD/CAL-VAL/SR/05/05/2015	
2. Publication Date	May, 2015	
3. Title	Calibration and Validation Site characterisation of INSAT-3D Satellite over Great Rann of Kutch and White Rann of Kutch Joint Campaign of SAC & IMD	
4. Type of Report	Scientific	
5. Number of pages	21	
6. Number of references	19	
7. Authors	SAC- Hiren Bhatt, R P Prajapati, Piyush Patel IMD-A.K.Sharma, A. K. Mitra, Rakesh Kumar, D. M. Hindia, and K. C. Modh	
8. Originating unit	CVD/ADVG/EPSA/SAC	
9. Abstract	This document describes the Site suitability for vicarious calibration of imager and over Great Rann of Kutch for INSAT-3D satellite. It was found that site spatial variability was a critical factor in site selection and sensor calibration. The comparison of TOA radiance computed for Visible & SWIR channels over Great Rann of Kutch and INSAT-3D satellite radiance matches as per expected.	
10. Key Words	Vicarious Calibration, INSAT-3D, Radiative transfer code, Visible, SWIR channel Radiance at TOA	
11. Security classification	Unrestricted	
12. Distribution statement	Among all concerned	

Contents

References

Abstract

Looking towards the advancements and popularity of remote sensing and an ever increasing need for the development of a variety of new and complex satellite sensors, it has become even more essential to continually upgrade the ability to provide absolute calibration of sensors. This article describes a simple procedure for post-launch calibration of INSAT-3D VIS and SWIR channels over land site (Great Rann of Kutch (GROK), Gujarat). The calibration exercise was carried out for three consecutive days (29th April to 2nd May 2015) to account for characterization errors or undetermined post-launch changes in spectral response of the sensor. The measurements of field reflectance of study site (area ~ 7 km x 3 km) in the wavelength range 325-2500 nm, along with atmospheric parameters (Aerosol Optical Depth, Total Columnar Ozone, Water Vapor) and sensor spectral response functions, were input to the 6S radiative transfer model to simulate radiance at top of the atmosphere (TOA) for VIS and SWIR bands. The uncertainty in vicarious calibration coefficients due to measured spatial variability of field reflectance along with due to aerosol types were also computed for the INSAT-3D imager. The results show that there is no indication of change in calibration coefficients for VIS and SWIR bands during these three days. .

Analysis shows that for clear sky days, the INSAT-3D imager underestimates TOA radiance in the VIS band by 2.5% and overestimates in the SWIR band by 4.2% with respect to 6S simulated radiance. For these bands, in the inverse mode, the 6S corrected surface reflectance was closer to field surface reflectance. It was found that site spatial variability was a critical factor in estimating change in sensor calibration coefficients and influencing uncertainty in TOA radiance for Great Rann of Kutch.

1. Introduction

With the advancement of remote sensing, the accurate characterization of the conversion of digital counts to radiance values, known as absolute calibration. Post-launch calibration is important to remote sensing because it enables a comparison of responses of pre-launch satellite sensors and the ability to monitor their changes over time, which improves the quality of satellite sensor and data products. Calibration and validation are essential activities to maintain the performance of the satellite sensors and its data products. Vicarious calibration provides a method for absolute calibration of satellite sensors using reference and accurate measurements of spectral reflectance from the ground instruments. This absolute calibration produces the calibration coefficients that can be replaced with pre-launch laboratory derived coefficients. Prior to launch, on-board calibration (Bruegge et al., 1993) and radiometric calibration (Bruegge et al., 1998) are the parts of calibration procedures but where the on-board calibration facility does not exist for the necessity of absolute calibration, in that case, a post-launch calibration is needed to compensate the degradation of the satellite sensor (Rao, 2001). A vicarious calibration is practise to monitor the radiometric performance of satellite sensor, which involves the computation of uncertainties in the calibration coefficients to correct the radiometric response of the satellite sensor (Thome et al., 1998). Vicarious calibration is a process to simulate the radiance value using field measurement of field reflectance and atmospheric parameters in the homogenous conditions to those at the satellite level. INSAT-3D satellite was launched on 26th July 2013 using an Ariane 5 ECA launch vehicle from Kourou, French, Guyana. It carries mainly two payloads, (1) 6-channels Imager and (2) 19-channels atmospheric sounder, which operate in visible to thermal infrared region. Vicarious calibration was performed to monitor the in-orbit degradation of INSAT-3D imager. This study details the post-launch vicarious calibration performed using high reflectance target site with uniform and flat terrain (Great Rann of Kutch) for VIS (0.55-0.75 μm) and SWIR (1.55-1.70 μm) channels of the INSAT-3D imager, for justification of post-launch changes in the sensor response. These channels have 1km spatial resolution and 30 minutes temporal resolution. The reflectance-based approach was used with field measured surface reflectance and measurements of atmospheric parameters (aerosol optical depth (AOD), total columnar ozone and water vapor) for three different days (30th April, 1st May and 2nd May 2015). These measured quantities along with spectral response function (pre-launch laboratory measured) were input to the 6S radiative transfer (RT) code for the simulation of TOA radiance for both the channels. The 6S simulated radiance was compared with the INSAT-3D imager derived radiance to compute the calibration coefficients for both the channels. The uncertainties due to various factors (e.g. measurements of surface reflectance,

selection of aerosol model, surface anisotropic effect and 6S model uncertainties) were computed for the vicarious calibration coefficients of INSAT-3D imager.

2. Site and Data

Attributing to their preferable stability of surface characteristics and atmospheric dynamics, pseudo-invariant sites are commonly used for sensor radiometric calibration, degradation monitoring and inter-comparisons (Chandra et al., 2010; Bouvet et al., 2014) especially for the satellite sensors without on-board calibration facilities. The Committee on Earth Observation Satellites (CEOS) Working group on Calibration and Validation identified several sites around the world (Teillet and Chandra, 2010) based on the selection criteria, such as low probability of atmospheric interruptions, high spatial homogeneity, weak directional effects, flat reflectivity spectrum etc. Calibration sites are never chosen randomly, and to be adequate they must satisfy a certain number of criteria (Scott et al., 1996; Slater et al., 1996; Slater et al., 1987; Teillet et al., 1997). Initially, a joint campaign (Cal/Val team) was carried out in the month of February 26-28, 2015 to find a suitable site for the purpose of calibration and validation and to get the information of uniformity, accessibility, useable area and local information of the site. Based on the above criteria, we have selected a desert site in Great Rann of Kutch (GROK), India.
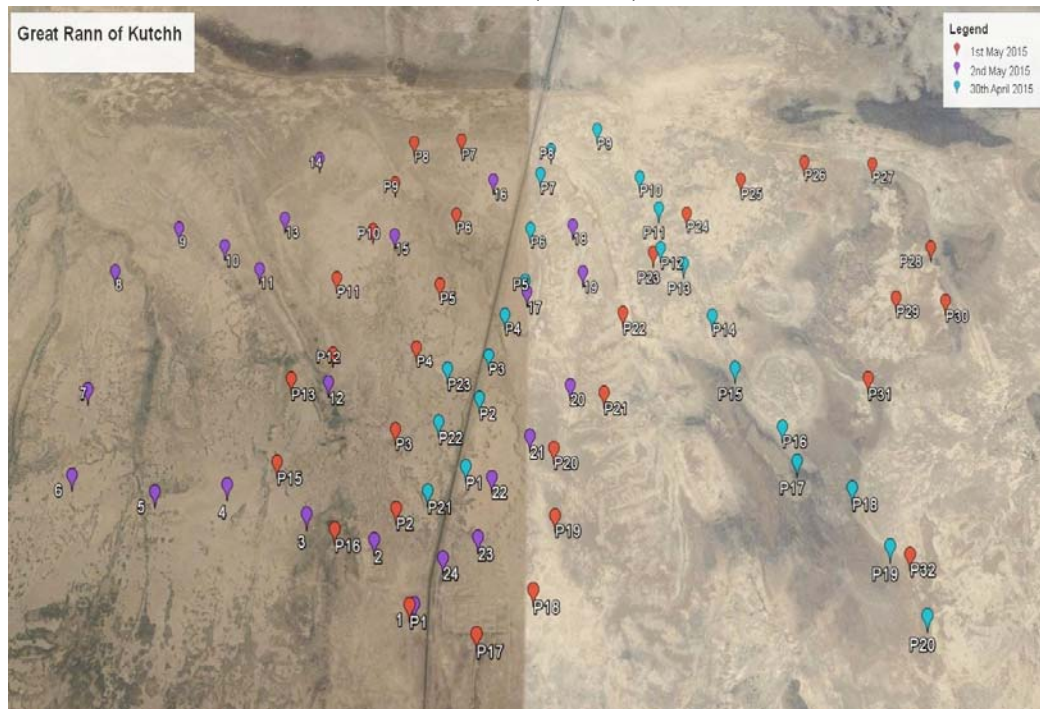
Figure 1: Calibration Site at Great Rann of Kutch including the data collection points.

Great Rann of Kutch (GROK) site characterised as high and uniform reflectance land, was chosen to carry out vicarious calibration. The experimental site is placed about 40 kilometres away from Bhuj, and between Khawda and Loriya, Gujarat. The site is accessible near to road on the way to Khawda. The centre of the site used for calibration is located at 23.52° N and 69.66° E. The area of the site presents a smooth and homogenous surface characterized by a good spatial uniformity, which is used for radiometric calibration of sensors with large foot print e.g. INSAT-3D imager. Figure-1 describes the location of calibration site along with the points where data are acquired.

In addition, we have collected the data on White Rann of Kutch (WROK) for second day of campaign (01st May, 2015). It is placed near Dhorado village, Bhuj, Gujarat.. Figure-2 describes the data acquisition points over WROK. Due to severe weather conditions, we were able to collect data on six points over WROK.

Figure 2: White Rann of Kutch along with data collection points for 01st May 2015.

Laboratory calibrated Analytical Spectral Device (ASD) Spectroradiometer was used for the measurements of field reflectance in the 7km x 3km region in the study site. Data have been collected at a distance of approximately every 500 meter. The retrieved daily mean surface reflectance of 3 days is shown in figure-3. The surface reflectance data was collected randomly within the site (7km x 3km). We covered a site daily for 90 minutes to cover the 3 consecutive images of INSAT-3D imager.
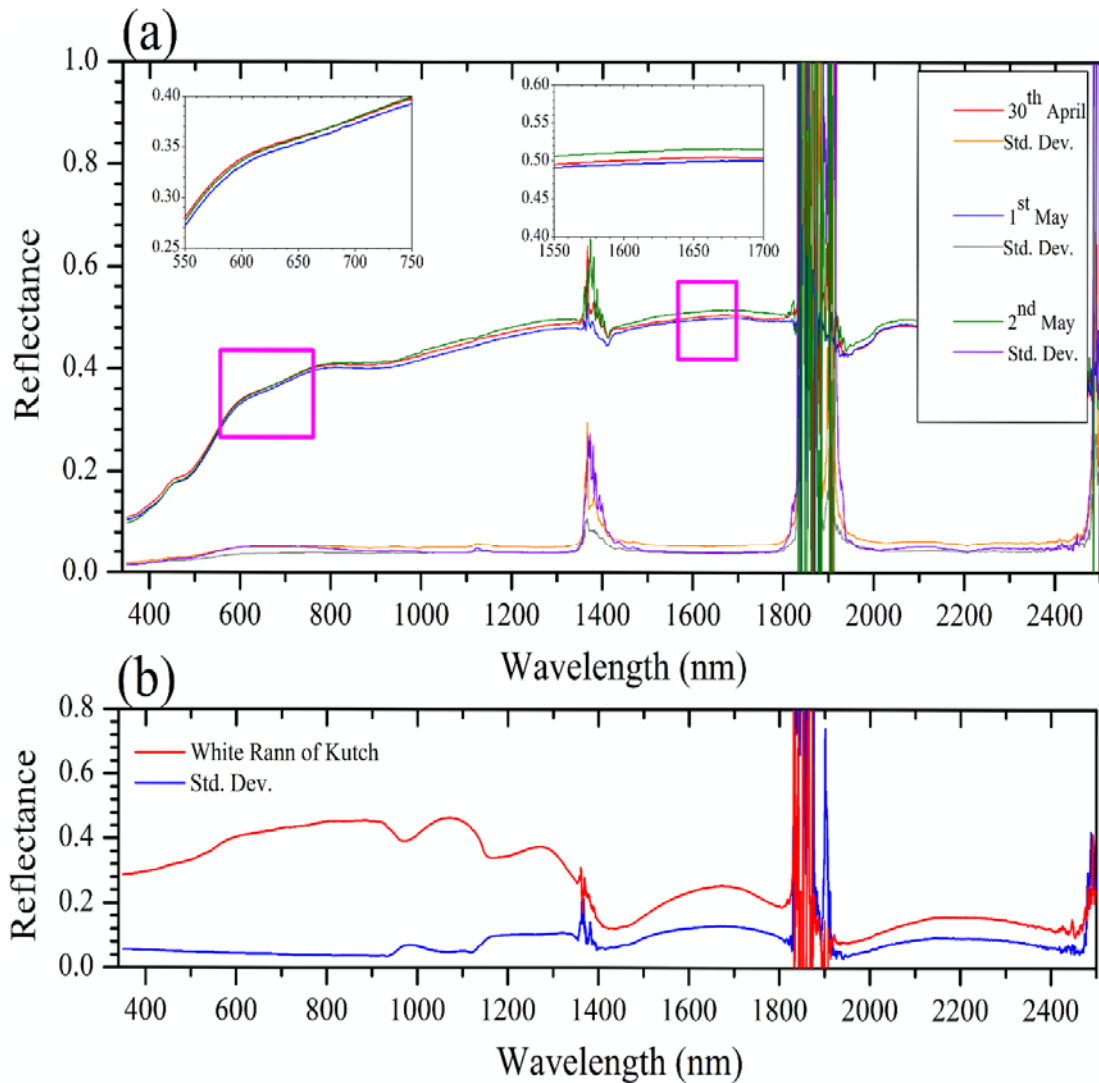
Figure 3(a) Three days daily mean variation of measured surface reflectance at GROK and (b) Mean surface reflectance at WROK.

Figure-3(a) shows the measured surface reflectance for the three different days over GROK and figure-3(b) shows the measured mean surface reflectance over WROK. Two distinct peaks due to water vapor absorption at 1380nm and high atmospheric absorption at 1800nm are the major reasons for the two noise points in the reflectance curves. We excluded the unreliable data from the figure-3 due to dust storm and high wind speed. Variation in surface reflectance is found to be very small (2.6% and 2.8%) in VIS as well as SWIR channel, which indicates the spatial homogeneity of the site selected for calibration of satellite sensors.

Radiometric spatial uniformity and temporal stability of targets are main issues to consider when using target site for the calibration and long-term radiometric control of satellite sensor data (Bannari et al., 2005). The optical characteristics of any target site can vary due to topography variation, surface moisture variation, cracks in the dry

surface that trap light, presence of vegetation, non-Lambertian behaviour of the surface increasing BRDF effects, as well as meteorological conditions. (Slater et al., 2004; Teillet et al., 1997; Thome et al., 2001). Radiometric spatial uniformity and temporal evolution of the GROK site is confirmed by calculating spatial and temporal Coefficient of Variation (CV) measurements using cloud-free INSAT-3D images over the site.
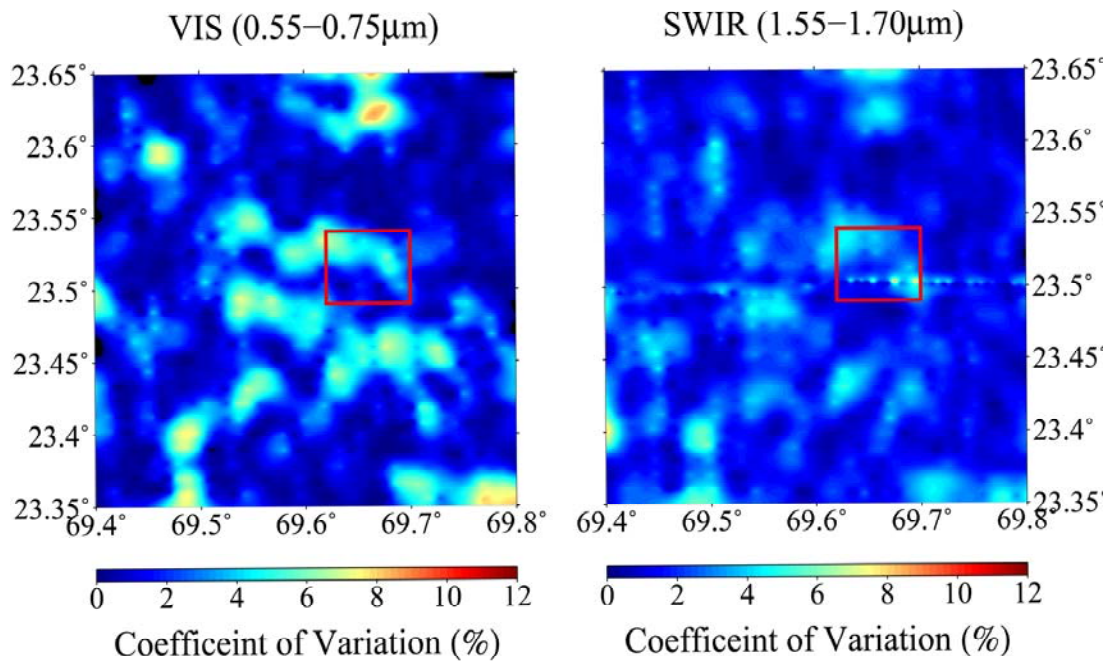
Figure 4: Image of the coefficient of variation calculated using 2km x 2km window in the two bands (VIS and SWIR) of the INSAT-3D image acquired on GROK on 1st May 2015 at 11:30 am. Red box shows the data collected site (7km x 3km).

The image is acquired on 1st May 2015 at 11:30 am. The study utilized VIS and SWIR bands. CV is defined by the ratio of the standard deviation over the average. In order to characterize the variability of the spatial homogeneity of the site, we set a 2 km x 2 km window size with a sampling step of 1 km. Figure-4 illustrates the result obtained using an INSAT-3D image acquired on 1st May 2015 at 11:30 am with the data collected site (6 km x 6 km) in red box. The CVs are found to be very similar for both the bands of the INSAT-3D imager. The highest values of CV is recorded 7.2% and 7.5% for VIS and SWIR, respectively, on the west side of the calibration site. The mean CV for the data collected site (red box) is found 5.1% and 4.2% for VIS and SWIR. This low variation indicates good site spatial homogeneity.

The temporal CV is evaluated for the three clear sky days using measured reflectance data over the site. Figure-5 indicates how the site surface reflectance has changed over these periods in both the bands (VIS and SWIR) of INSAT-3D. According to this figure, the variation of CV is low, on the order of 11% in VIS and

9% in SWIR. These results indicate that the Great ROK site undergoes very small changes to its surface due to variations in meteorological conditions that can be quite variable. The aerosol optical depth, total columnar ozone, and column water vapor are measured using Microtops-II Sunphotometer and Ozone monitor respectively at every 1km interval.
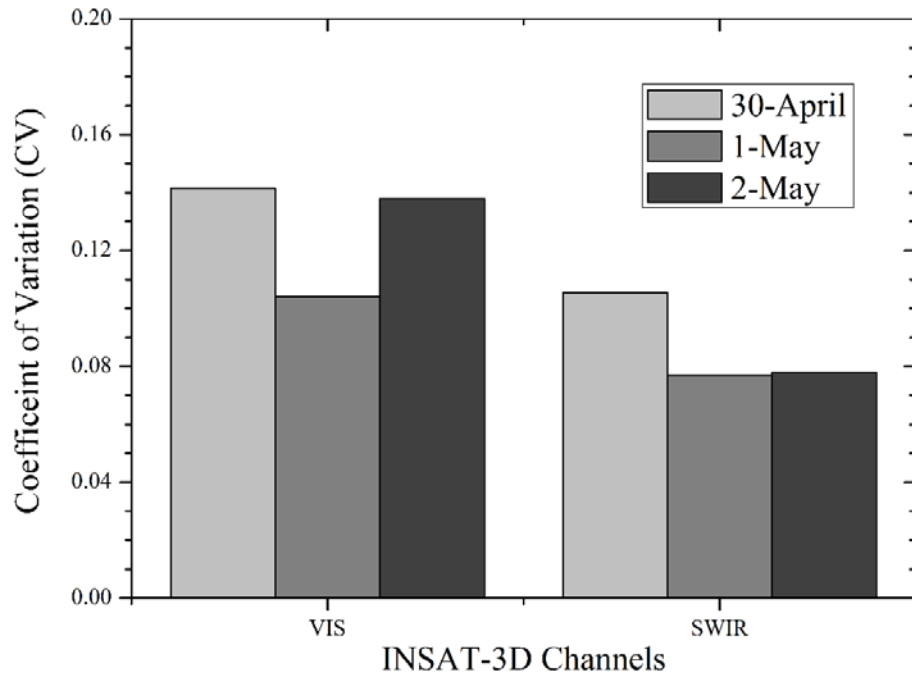
Figure 5: Coefficient of variation over GROK for three different days.

3. Methodology

In this study, vicarious calibration was performed using reflectance based approach, which was provided by Slater et al., (1987). This technique has been successfully used for satellite's sensor calibration (Biggar et al., 1991; Gellaman et al., 1993). In this technique, the INSAT-3D imager derived radiance is compared with 6S simulated TOA radiance. The vicarious radiometric calibration depends on measuring the surface reflectance, path from the sun to earth's surface and earth's surface to sensor and atmospheric optical thickness over a calibration site at the time of satellite overpass. These measurements are used as an input for RT code to simulate an absolute radiance at the sensor level. The field measurements are used to define the spectral directional reflectance of the surface and the spectral optical depth that are used to describe the aerosol and molecular scattering effect in the atmosphere (Gellman et al., 1991) and along with this we used columnar water vapor

include the water vapor absorption effect. The detailed values of atmospheric parameters are given in table-1.

Table 1: daily mean value of atmospheric parameters over GROK and WROK (e.g. Aerosol optical Depth, Total Ozone Content, Water Vapor).

Days	AOD@550 nm	Total ozone content (Dobson)	Water Vapor (g cm^{-2})
30th April 2015	0.533	323.4	1.01
1st May 2015	0.520	305.49	0.62
1st May 2015 (White ROK)	0.490	304.43	0.78
2nd May 2015	0.406	305.22	0.47
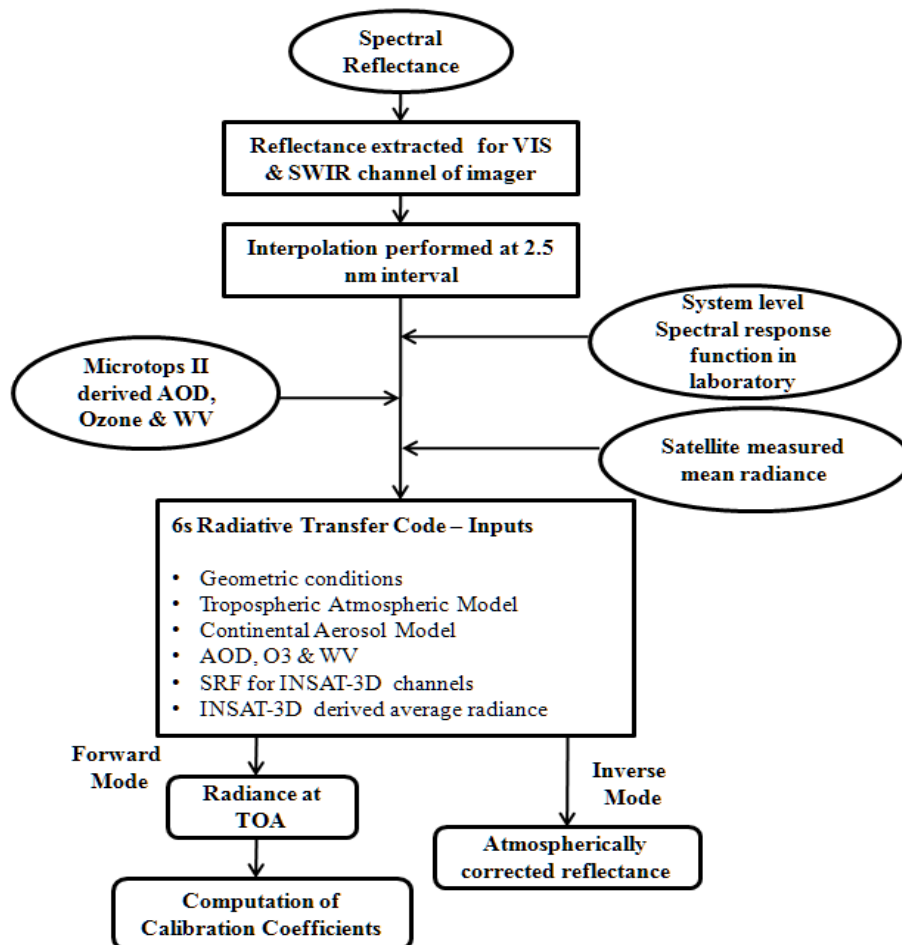
Figure 6: Flow chart for the simulation of TOA radiance and estimation of calibration coefficient.

We have used 6S RT code to compute the radiance using ground measurements, which predicts the satellite signal at TOA level using field

measurements. 6S RT model is a physically based model, not specified for particular satellite. In addition, 6S RT model utilizes gaseous absorption and scattering by aerosols and molecules. 6S performs better for atmospheric scattering as compared to other RT models (Markham et al., 1992). 6S model was formulated for the atmospheric correction in the short wavelengths. Figure-6 describes the flow chart to simulate radiance at TOA and vicarious calibration coefficient. The US 62 standard atmosphere profile provides the profiles of water vapor, ozone, pressure and temperature up to 100km, at discrete intervals of 34 layers in the 6S RT model (Vermote et al., 2006).

For the selection of optimum aerosol model, we analysed relation between AOD and Angstrom exponent ($\alpha_{440-870\ nm}$) (Kaskaoutis et al., 2007) because two aerosol properties helps to characterise the aerosol types (Holben et al., 2001). In this technique, some threshold values are used to discriminate the aerosol types, which may modify with location, aerosol range and aerosol characteristics (Kaskaoutis et al., 2009). In the present study, we have adopted same threshold values as Kaskaoutis et al. (2009) used over Hyderabad. Total five different types of aerosols are identified using this analysis (e.g. DD=desert dust, MA=mixed aerosol, AA=anthropogenic aerosol, BB=biomass burning, CC=clean conditions). Figure-7 shows the percentage variation of different aerosols over GROK and WROK for the study period.
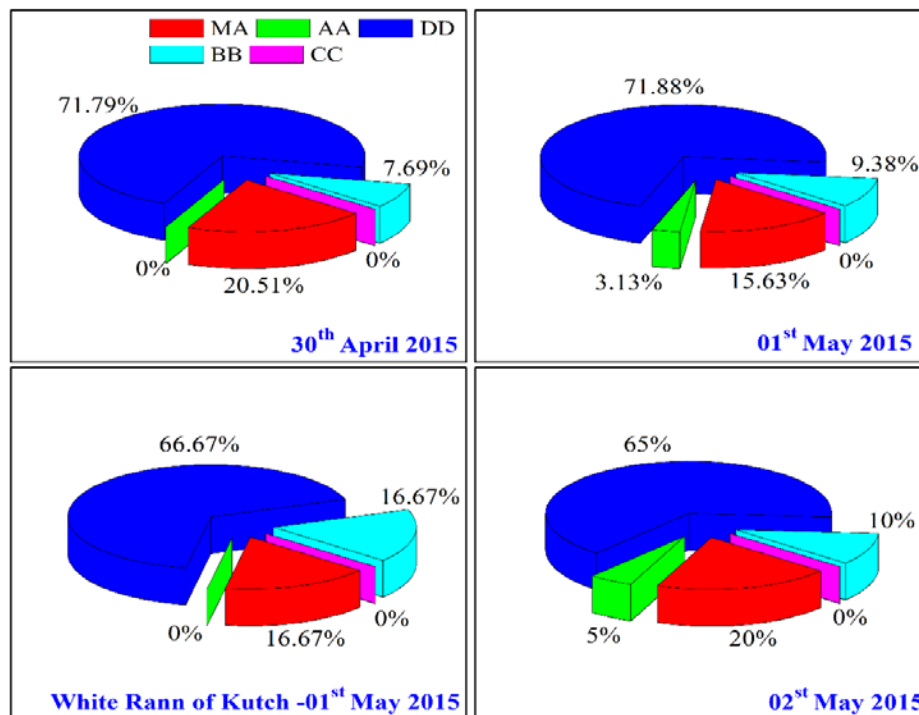
Figure 7: Daily percentage variation of different types of aerosols over GROK and WROK sites.

The analysis suggests that the both the sites are experiencing the dust (>65%) for all three-days and because of that continental aerosol model (a composite with

0.70% of dust like, 0.29% of water-soluble and 0.01% of soot component) has been chosen for the radiance simulation in 6S code. Continental aerosol model is the basic model over the land site and it is assumed that there is no impact of marine and polluted urban aerosols over both the sites. The aerosol data with continental aerosol model were used as an input of 6S RT code. We have used pre-launch laboratory measurements of spectral response function as an input, which is shown in figure-8 (Murali and Padmanabhan, 2011). Both the SRF and ground reflectance data are resampled to 2.5 nm intervals using spline interpolation method.
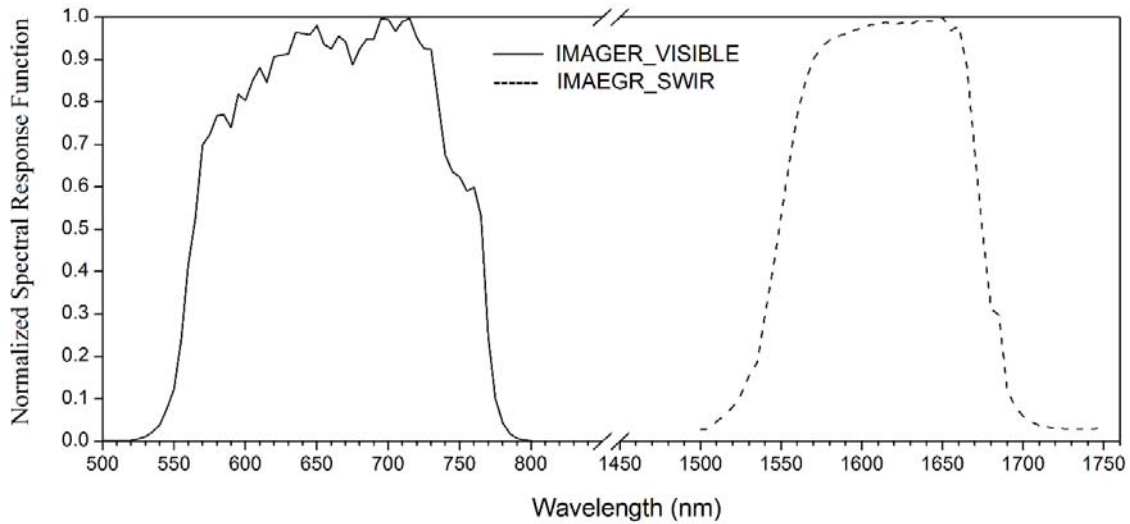
Figure 8: Pre-launch laboratory measurements of spectral response function for VIS and SWIR channels of INSAT-3D.

6S RT model provides an output in the form of TOA radiance, which is divided by the corresponding radiance observed by the INSAT-3D imager to yield vicarious calibration coefficients.

4. Results and Discussions

4.1. Regression Analysis

The 6S simulated TOA radiance was compared with the INSAT-3D imager radiance. The result of combined linear regression along with daily linear regression for VIS and SWIR over GROK are shown in figure 9 and 10. The good statistical agreement was observed between satellite-derived radiance and simulated radiance, with R^2 values of 0.9 0and 0.97 and with RMSE values of 2.06 $Wm^{-2}sr^{-1}\mu m^{-1}$ and 0.37 $Wm^{-2}sr^{-1}\mu m^{-1}$ for the VIS and SWIR channels respectively. The bias between satellite-derived radiance and 6S simulated radiance is minimal, with the values of 1.74 Wm^{-}

$^2sr^{-1}\mu m^{-1}$ and 0.25 $Wm^{-2}sr^{-1}\mu m^{-1}$ for VIS and SWIR channels respectively. INSAT-3D imager underestimates the radiance values by 2.5% in the VIS and it overestimates the radiance value by 4.2% in the SWIR channel.
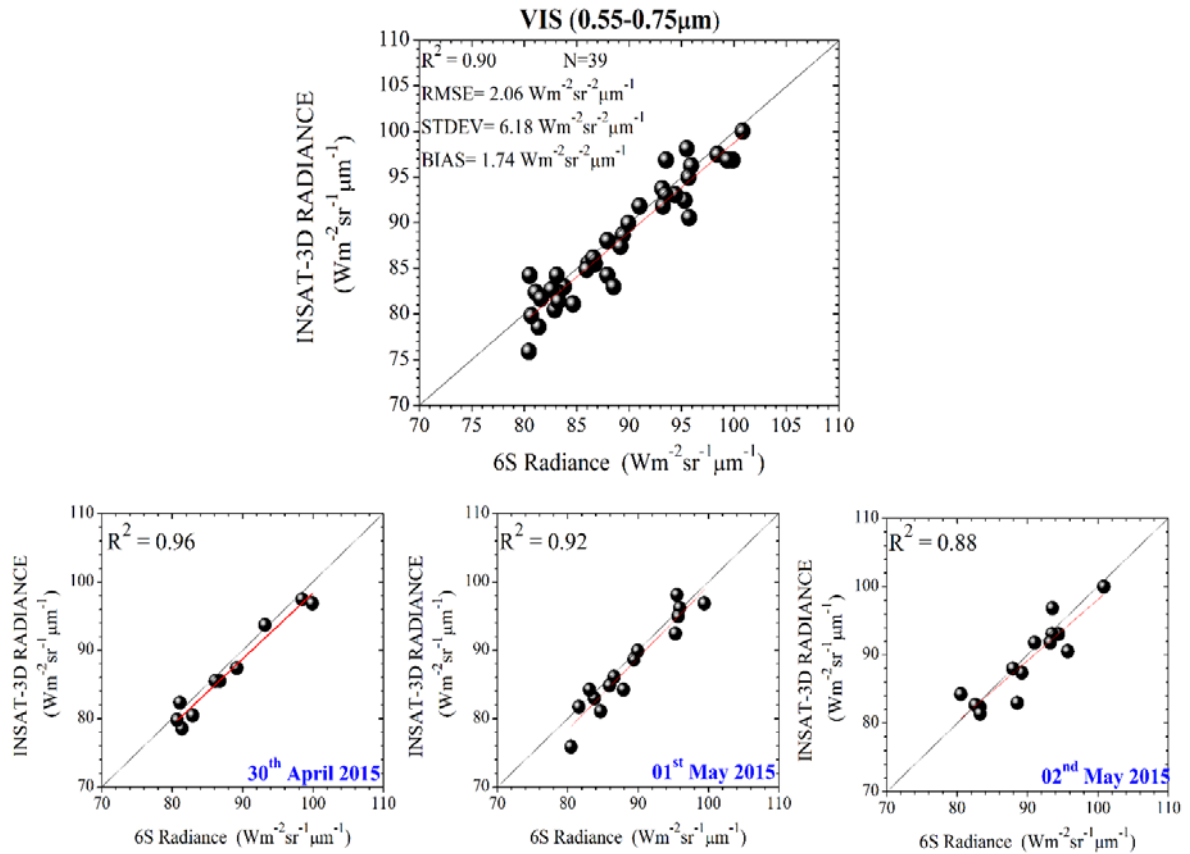
Figure 9: The combine linear regression between INSAT-3D measured and 6S simulated Radiance over GROK for VIS channel.

Summary of the statistical analysis for the comparison between INSAT-3D measured and 6S simulated radiance are shown in table-2.

Table 2: Summary of Statistics for regression analysis

Channels	R^2	Bias	RMSE	Standard deviation
VIS (0.55-0.75 μm)	0.90	1.74 $Wm^{-2}sr^{-1}\mu m^{-1}$	2.06 $Wm^{-2}sr^{-1}\mu m^{-1}$	6.18 $Wm^{-2}sr^{-1}\mu m^{-1}$
SWIR (1.55-1.70 μm)	0.97	0.25 $Wm^{-2}sr^{-1}\mu m^{-1}$	0.37 $Wm^{-2}sr^{-1}\mu m^{-1}$	1.40 $Wm^{-2}sr^{-1}\mu m^{-1}$
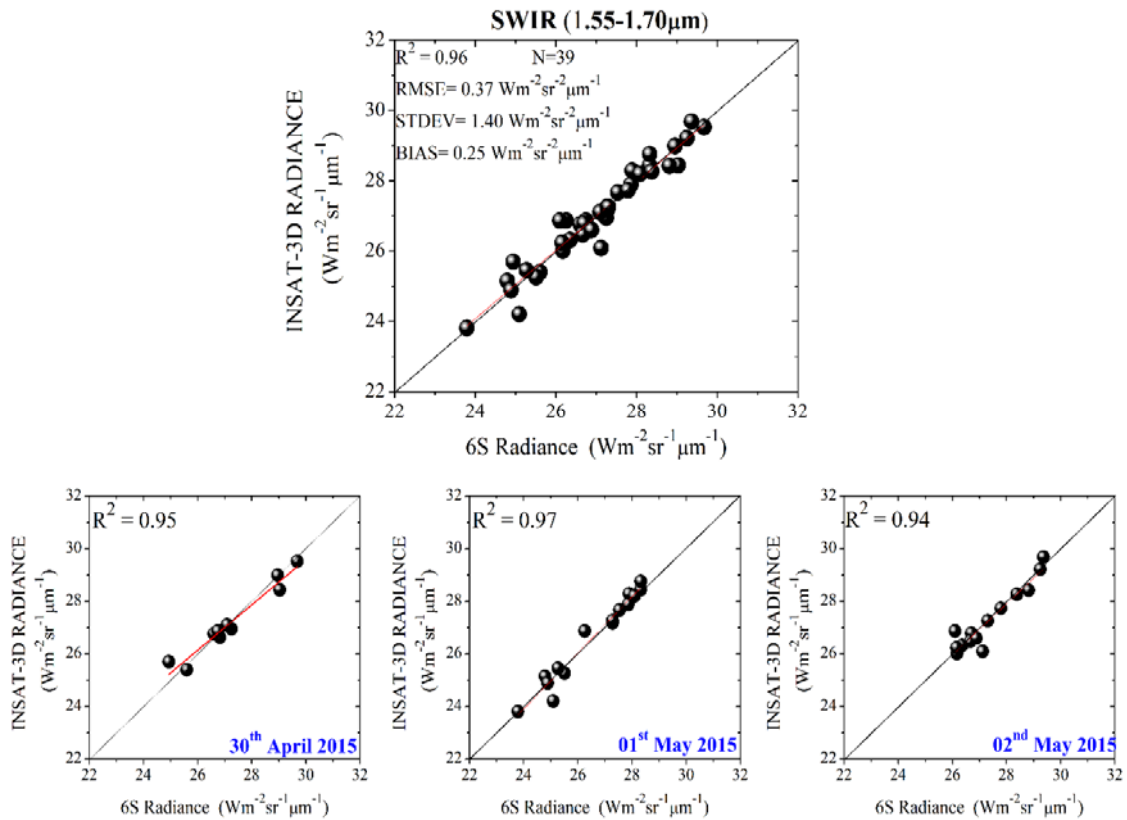
Figure 10: The combine linear regression between INSAT-3D measured and 6S simulated Radiance over GROK for SWIR channel.

It has been found that the differences between satellite and 6S RT derived radiance at VIS channel are relatively large compared to SWIR channel due to the differences in radiance range. Figure-11 describes the regression between INSAT-3D measured and 6S simulated radiance over WROK.
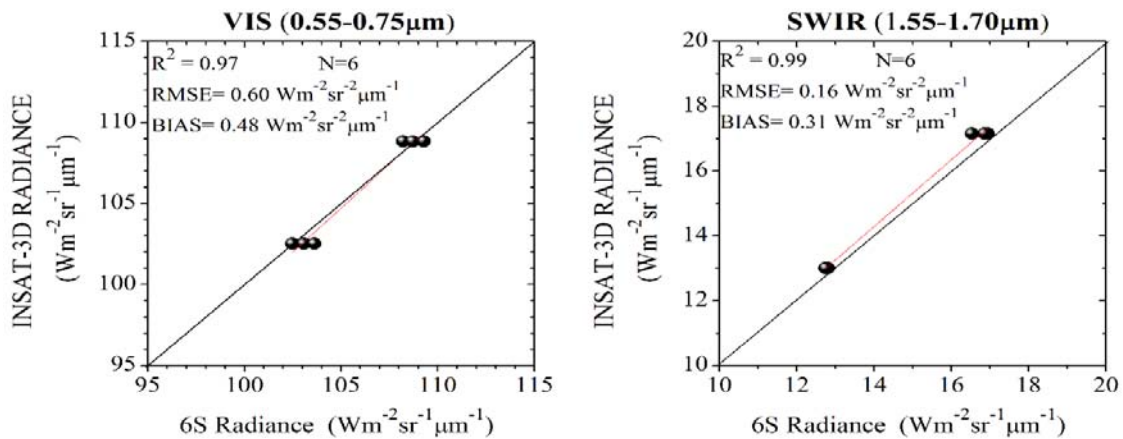
Figure 11: Regression analysis between INSAT-3D and 6S derived radiance over WROK for both VIS and SWIR.

The good statistical agreement was observed between satellite-derived radiance and simulated radiance, with R^2 values of 0.97 0and 0.99 and with RMSE values of 0.6 $Wm^{-2}sr^{-1}\mu m^{-1}$ and 0.16 $Wm^{-2}sr^{-1}\mu m^{-1}$ for the VIS and SWIR channels respectively. The bias between satellite-derived radiance and 6S simulated radiance is minimal, with the values of 0.48 $Wm^{-2}sr^{-1}\mu m^{-1}$ and 0.31 $Wm^{-2}sr^{-1}\mu m^{-1}$ for VIS and SWIR channels respectively. The analysis indicates the INSAT-3D measured radiance is underestimated the radiance values by 2.5% for VIS channel, whereas INSAT-3D measured radiance is overestimated the radiance value by 4.2% for SWIR channel. The differences between satellite and 6S RT derived radiance at VIS channel are relatively large compared to SWIR channel due to the differences in radiance range. The radiance variation from figure-11 indicates the INSAT-3D underestimates the radiance values in VIS channel, whereas it overestimates the radiance values in SWIR channel. It is observed that the mean differences between satellite measured and 6S simulated radiance are 1.06 $Wm^{-2}sr^{-1}\mu m^{-1}$ for VIS and -0.49 $Wm^{-2}sr^{-1}\mu m^{-1}$ for SWIR channels.
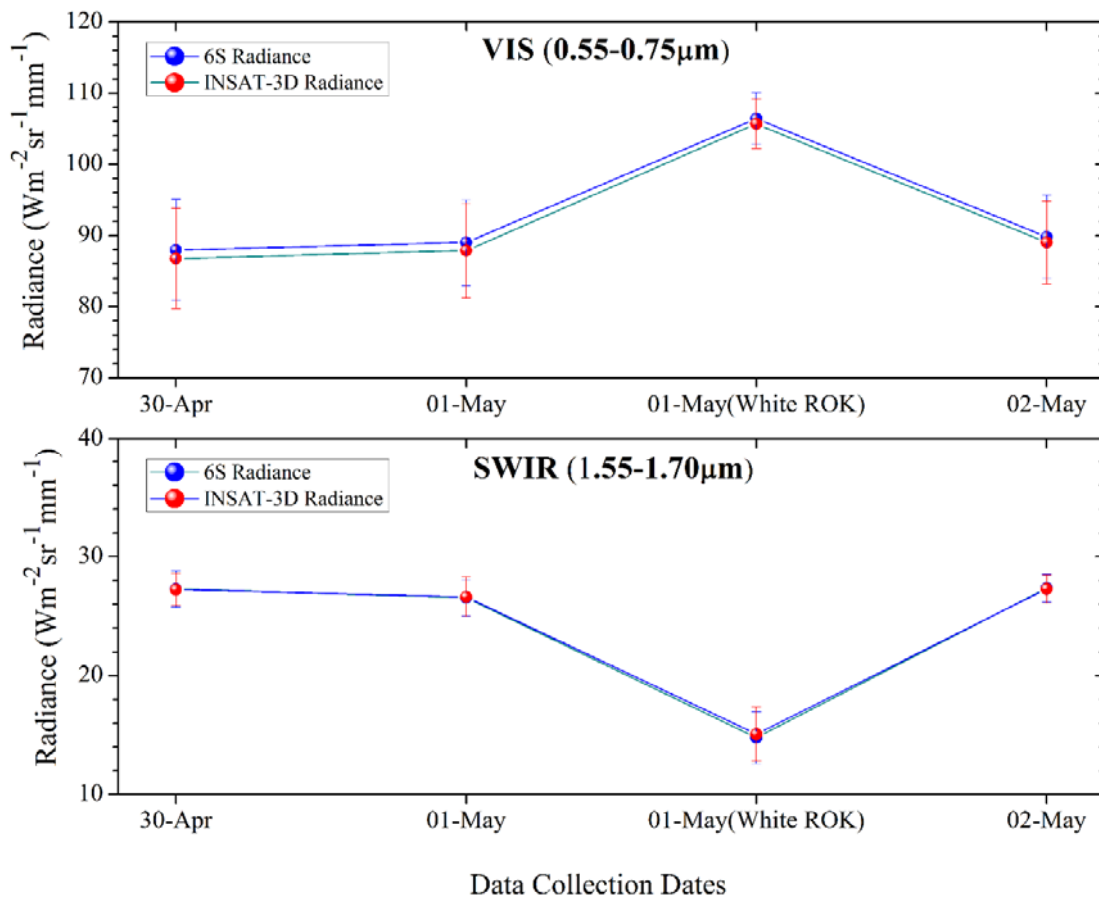
Figure 12: Daily variation of radiance from INSAT-3D and 6S simulated for VIS and SWIR channels.

4.2. Estimation of Vicarious Calibration Coefficient

Table-3 describes the mean TOA radiance, surface reflectance, and vicarious calibration coefficient derived from measurements at the GROK and WROK sites for the study period. From table- 3, the mean values of simulated and satellite observed radiance are highly comparable throughout the two channels of INSAT-3D imager. The differences between simulated and observed radiance are very small which is due to the intrinsic variability and meteorological variability of the sites. It was observed that radiance values for the SWIR channels are more comparable than VIS.
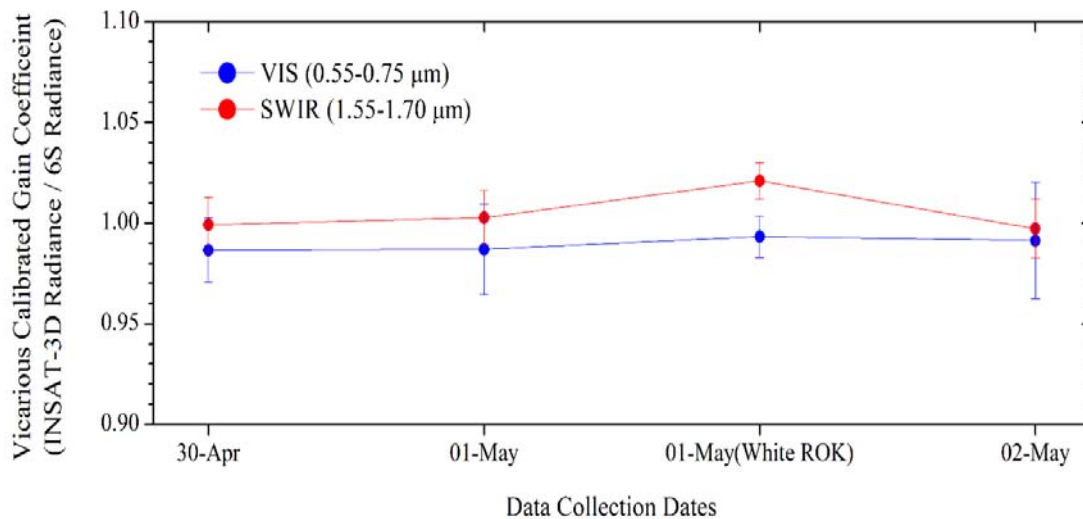
Figure 13: Estimated vicarious calibration gain coefficient over GROK and WROK.

The vicarious calibration coefficient is the ratio of 6S simulated radiance and satellite observed radiance in the case of INSAT-3D imager. For an ideal case, if there is no degradation in the sensor during launch and ground and atmosphere are absolutely characterized and have an accurate RT code, simulated TOA radiance should precisely match with satellite observed radiance. It means the ratio of simulated to observe radiance should be unity. In practice it is not possible, there are uncertainties in field reflectance and atmospheric measurements, modelling uncertainties in the RT code.

Figure- 12 describes the ratio of the TOA radiance simulated using ground measured data to the INSAT-3D imager derived radiance for each channel and each day along with average value. The vicarious calibration coefficient data for INSAT-3D imager describes minor changes in the calibration of INSAT-3D imager for both the channels and the change is slightly more in SWIR channel with respect to VIS. The

standard deviation of the calibration coefficient is less than 2% for each channel in figure-12. The ratio is decreasing with wavelength but generally, ratio does not depend on the wavelengths. This study aims towards the methodology followed and indicates that the errors (< 5%) lie within the radiometric uncertainty. The relative percentage error at both the channels for all days describes in Table-3. The relative errors are found to be less than 3%.

Table 3: The values of radiance from INSAT-3D and 6S along with relative error and calibration coefficients for both the channels (VIS and SWIR) for all three days over both GROK and WROK sites.

Date	Channels	INSAT-3D Radiance $(Wm^{-2}sr^{-1}\mu m^{-1})$	6S Simulated Radiance $(Wm^{-2}sr^{-1}\mu m^{-1})$	Relative Error in Radiance (%)	Calibration Coefficient
30th April 2015	VIS	86.76	87.95	1.37	0.986
	SWIR	27.27	27.23	0.12	0.999
1st May 2015	VIS	87.88	89.01	1.28	0.986
	SWIR	26.54	26.62	-0.29	1.002
1st May 2015 (WROK)	VIS	105.68	106.40	0.68	0.993
	SWIR	14.77	15.08	-2.07	1.021
2nd May 2015	VIS	89.01	89.82	0.90	0.991
	SWIR	27.36	27.28	0.27	0.997

The relatively small biases in the VIS and SWIR channels are well in agreement with the INSAT-3D imager radiometric uncertainty. The noted values were found to be consistent, which indicate good calibration stability of INSAT-3D imager.

5. Conclusion

In this study, post-launch calibration was carried out for the VIS and SWIR channels of INSAT-3D imager over the Great Rann of Kutch and White Rann of Kutch sites. The TOA radiance was simulated by 6S RT model using ground measurements. The conclusions based on this study are summarized below:

1) The present study concludes that GROK site is the preferred site for post-launch calibration due to its accessibility, high degree of homogeneity, which helps to derive precise vicarious calibration coefficients.

2) The spatial and temporal variability of site is quantified by the variation of mean reflectance and coefficient of variation. The mean reflectance varies by 2.6% for VIS

and 2.8% for the SWIR channels, the CV was found to be lesser for the GROK site (2%-3%) in both the channels of INSAT-3D imager.

3) The 6S simulated radiances are well comparable with the INSAT-3D imager measured radiance for all three dates over GROK and for WROK.

4) The close agreement was observed between simulated and satellite measured TOA radiance. The mean difference in vicarious calibration coefficients for the INSAT-3D imager is less than 3% for both the channel for all three days over GROK site.

5) Uncertainty in TOA radiance due to selection of aerosol model is much less. The uncertainty is found to be ~0.5% for desert model and ~0.7% for urban model with respect to continental model.

6) The estimated overall uncertainties in the calibration coefficients are found to be 3.63% in VIS and 4.11% in SWIR channels of INSAT-3D imager.

7) INSAT-3D measured radiance is underestimated with respect to the 6S radiance value by 2.5% for VIS channel, whereas it is overestimated by 4.2% for SWIR channel.

Acknowledgement

References

C. J. Bruegge, A. E. Stiegman, R. A. Rainen, and A. W. Springsteen. (1993). Use of Spectralon as a diffuse reflectance standard for in-flight calibration of earth-orbiting sensors. *Optical Engineering*. 32. pp. 805–814.

C. J. Bruegge, V. G. Duval, N. L. Chrien, R. P. Korechoff, B. J. Gaitley, and E. B. Hochberg. (1998). MISR prelaunch instrument calibration and characterization results. *IEEE Transactions on Geoscience and Remote Sensing*. 36. pp. 1186–1198.

C. R. N. Rao. (2001). Implementation of the Post-Launch Vicarious Calibration of the GOES Imager Visible Channel. (Camp Springs, MD: NOAA Satellite and Information Services (NOAA/NESDIS)), http://www.ospo.noaa.gov/Operations/GOES/calibration/vicarious-calibration.html.

K. Thome, K. S. Schiller, J. Conel, K. Arai, S. Tsuchida. (1998). Results of the 1997 Earth Observing System Vicarious Calibration joint campaign at Lunar Lake Playa, Nevada (USA). *Metrologia*. 35. pp. 631–638.

P. N. Slater, S. F. Biggar, R. G. Holm, R. D. Jackson, Y. Mao, M. S. Moran, J. M. Palmer, B. Yuan. (1987). Reflectance- and radiance-based methods for the in-flight absolute calibration of multispectral sensors. *Remote Sensing of Environment.* 22. pp. 11–37.

S. F. Biggar, M. C. Dinguirard, D. I. Gellman, P. Henry, R. D. Jackson, M. S. Moran, P. N. Slater. (1991). Radiometric calibration of SPOT 2 HRV: a comparison of three methods. *Proc. SPIE.* 1493. pp. 155-162.

D. I. Gellman, S. F. Biggar, M. C. Dinguirard, P. J. Henry, M. S. Moran, K. J. Thome, P. N. Slater,. (1993). Review of SPOT-1 and -2 Calibrations at White Sands from Launch to the Present. *Proc. SPIE.* 1938. pp. 118-125.

D. I. Gellman, S. F. Biggar, P. N. Slater, and C. J. Bruegge. (1991). Calibrated intercepts for solar radiometers used in remote sensor calibration. *Proc. SPIE.* 1493. pp. 19–24.

B. L. Markham, R. N. Halthore, S. J. Goetz. (1992). Surface reflectance retrieval from satellite and aircraft sensors: results of sensor and algorithm comparison during FIFE. *Journal of Geophysical Research.* 97 (D17). pp. 18785-18795.

E. Vermote, D. Tanre, J. L. Deuze, M. Herman, J. J. Morcrette, S. Y. Kotchenova. (2006). Second Simulation of Satellite Signal in the Satellite Spectrum (6S). 6S User Guide Version 3. University of Maryland.

Hess M., Koepke P., and Schultz I., 1998. Optical properties of aerosols and clouds: The software package OPAC. Bull. Am. Meteorol. Soc., 79, 831–844.

Schuster G.L., Dubovik O., Holben, B.N., 2006. Angstrom exponent and bimodal aerosol size distributions. J. Geophys. Res., 111: D07207, doi:10.1029/2005JD006328.

K. R. Murali, and D. Padmanabhan, "Spectral response details, INSAT-3D imager (FM)-V-2.0," Space Applications Centre, ISRO, Ahmedabad, Gujarat, India, Technical Report, Doc No: SAC/EOSG/GPID/30/03/2011/17, 2011.

F. E. Nicodemus, J. C. Richmond, J. J. Hsia, I. W. Ginsberg, T. Limperis. (1977). Geometrical considerations and nomenclature for reflectance. *Natl. Bur. Stand. Rep.* NBS MN-160. 52 pp.

Gao, H. L., X. F. Gu, T. Yu, X. Y. Li, T. H. Cheng, H. Gong, and J. G. Li. 2009. "Radiometric
Calibration for HJ-1a Hyper-Spectrum Imager and Uncertainty Analysis." *Acta Photonica Sinica,* 38: 2826–33.

S. F. Biggar, P. N. Slater, and D. I. Gellman. (1994). Uncertainties in the in-flight calibration of sensors with reference to measured ground sites in the 0.4 to 1.1 _m range. *Remote Sensing of Environment.* 48. pp. 242–252.

P. N. Slater, S. F. Biggar, J. M. Palmer, K. J. Thome. (1995). Unified approach to pre- and in-flight satellite sensor absolute radiometric calibration. *Proc. SPIE.* 2583. pp. 130–141.

K. Thome, B. Markham, J. Barker, P. Slater, S. Biggar. (1997). Radiometric calibration of Landsat. *Photogramm. Eng. Remote Sensing.* 63. pp. 853–858.

J. Yang, P. Gong, R. Fu, M. Zhang, J. Chen, S. Liang, B. Xu, J. Shi, R. Dickinson. (2013). The role of satellite remote sensing in climate change studies. *Nature Climate Change.* 3. pp. 875–883.

A. K. Sharma et al., (2014), calibration /validation of INSAT-3D satellite: First joint campaign in Jaisalmer during 14-23, December, 2013, Meteorological monograph. ESSO/IMD/SATMET/01/2014/7.